Journal of Nuclear Medicine, published on February 14, 2020 as doi:10.2967/jnumed.119.240895

Quantification of PD-L1 expression with [^{18}F]BMS-986192 PET/CT in patients with advanced stage non-small-cell lung cancer

Authors

Marc C Huisman[1]*, Anna-Larissa N Niemeijer[2]*, Albert D Windhorst[1], Robert C Schuit[1], David Leung[3], Wendy Hayes[3], Alex Poot[1], Idris Bahce[2], Teodora Radonic[4], Daniela E Oprea-Lager[1], Otto S Hoekstra[1], Erik Thunnissen[4], N. Harry Hendrikse[1], Egbert F Smit[2,5], Adrianus J de Langen[2,5], Ronald Boellaard[1]

*equally contributed to this manuscript

Author's affiliations

Departments of [1]Radiology & Nuclear Medicine and [2]Pulmonary Diseases, Cancer Center Amsterdam, Amsterdam UMC, Vrije Universiteit Amsterdam, De Boelelaan 1117, 1081 HV Amsterdam, The Netherlands.

[3]Bristol-Myers Squibb Research and Development, Route 206 & Province Line Rd., Princeton, NJ 08543, USA.

[4]Department of Pathology, Cancer Center Amsterdam, Amsterdam UMC, Vrije Universiteit Amsterdam, De Boelelaan 1117, 1081 HV Amsterdam, The Netherlands.

[5]Department of Thoracic Oncology, Netherlands Cancer Institute, Plesmanlaan 2, 1066 CX, Amsterdam, The Netherlands.

First/corresponding author

Marc Huisman

De Boelelaan 1117, 1081 HV Amsterdam, The Netherlands

Phone:+31204445162/Fax:+31204443090

Email: m.huisman@vumc.nl

Potential conflicts of interest: DL and WH are employees and stock holders of BMS.

Financial support: not applicable.

Word count: 4003

Running title: Quantification of PD-L1 expression

Abstract

The aim of this work was to quantify the uptake of [^{18}F]BMS-986192, a PD-L1 adnectin PET tracer, in patients with non-small-cell lung cancer (NSCLC). To this end, plasma input kinetic modeling of dynamic tumor uptake data with online arterial blood sampling was performed. In addition, the accuracy of simplified uptake metrics such as standardized uptake value (SUV) was investigated.

Methods: Data from a study with [^{18}F]BMS-986192 in patients with advanced stage NSCLC eligible for nivolumab treatment were used if a dynamic scan was available and lesions were present in the field of view of the dynamic scan. After injection of [^{18}F]BMS-986192, a 60-minutes dynamic PET-CT scan was started, followed by a 30-min whole body PET-CT scan. Continuous arterial and discrete arterial and venous blood sampling were performed to determine a plasma input function. Tumor time activity curves were fitted by several plasma input kinetic models. Simplified uptake parameters included tumor to blood ratio as well as several SUV measures.

Results: Twenty two tumors in nine patients were analyzed. The arterial plasma input single-tissue reversible compartment model with fitted blood volume fraction seems to be the most preferred model as it best fitted 11 out of 18 tumor time activity curves. The distribution volume V_T ranged from 0.4 to 4.8 mL·cm^{-3}. Similar values were obtained with an image derived input function. From the simplified measures, SUV normalized for body weight (SUV_{BW}) at 50 and 67 minutes post injection correlated best with V_T, with an $R^2 > 0.9$.

Conclusion: A single tissue reversible model can be used for the quantification of tumor uptake of the PD-L1 PET tracer [^{18}F]BMS-986192. SUV_{BW} at 60 minutes post injection, normalized for body weight, is an accurate simplified parameter for uptake assessment of baseline studies. In order to assess its predictive value for response evaluation during PD-(L)1 immune checkpoint inhibition further validation of SUV against V_T based on an image derived input function is recommended.

Key words: PD-L1 expression, PET/CT, kinetic modeling, immune checkpoint inhibitors

Introduction

Non-small-cell lung cancer (NSCLC) has the highest mortality rate of solid tumors worldwide *(1)*. Over the last few years, treatment with immune checkpoint inhibitors (ICIs) has improved both progression free survival and overall survival in these patients *(2-4)*. Selecting patients who benefit most from ICIs treatment remains challenging. Tumor PD-L1 expression as measured by immunohistochemistry, is predictive for response and survival to some extent *(2)* and *(5)*. However, only approximately 40% of all programmed cell death-ligand 1 (PD-L1) positive patients respond to therapy, whereas 10% of the PD-L1 negative patients show a favorable response to ICIs *(6).* These differences may be explained by the heterogeneity of PD-L1 expression in tumors *(7)*. Moreover, tumor microenvironment, tumor mutational burden, activated oncogenic pathways and neoantigen presentation are only some of the additional factors that might influence the response to the immunotherapy *(8-10)*. Positron emission tomography (PET) can be used for in vivo visualization of specific molecular targets *(11)*.

Recently, 18F-BMS-986192 (an ^{18}F-labeled anti–PD-L1 Adnectin) was introduced to visualize PD-L1 expression in NSCLC. In vivo PET imaging demonstrated PD-L1 expression in mice implanted with PD-L1 (+) L2987 xenograft tumors along with radioligand binding blocked in a dose-dependent manner *(12)*. Subsequently, a proof-of-principle study showed that in vivo molecular imaging of PD-L1 is feasible and safe in patients with NSCLC *(13)*. Tumors expressing ≥50% PD-L1 expression had a higher uptake of 18F-BMS-986192 than lesions expressing less than 50% PD-L1 expression and responding lesions tended to have higher uptake of 18F-BMS-986192. Additionally, heterogeneity in uptake both between and within patients was demonstrated, suggesting a potential role for 18F-BMS-986192 PET to serve as a clinical biomarker. This may explain why a subset of tumor PD-L1 negative patients responds to ICIs.

The aim of this study was to identify the optimal pharmacokinetic model to quantify 18F-BMS-986192 kinetics in patients with NSCLC. To this end, kinetic modeling of dynamic tumor uptake data was performed with arterially sampled blood as input function. In addition, the applicability of simplified uptake metrics, such as SUV, was investigated.

Materials and Methods

Patients

Data were derived from a clinical trial (EUDRACT number 2015-004760-11 (*14*)). In this trial, 13 patients with advanced NSCLC eligible for nivolumab (PD-1 inhibitor) treatment were included. All patients were ICI naive. Inclusion and exclusion criteria are provided in *(13).* Only patients with a dynamic scan and lesions in the field of view were included in this analysis. This study was approved by the local Institutional Review Board (Medical Ethics Committee of the Amsterdam University Medical Centre, location VU University Medical Centre, Amsterdam) and conducted in accordance with the Declaration of Helsinki. Written informed consent was obtained prior to study enrollment in all human participants.

Biopsies

Ten biopsy samples were obtained before start of the scans. In three patients, archival material was used (range 12-20 months before start of nivolumab). PD-L1 immunohistochemistry was performed using the DAK 28.8 antibody *(15)* and PD-L1 expression was assessed as the percentage of tumor cells showing positive cell membrane staining for PD-L1 (tumor proportion score). Total PD-L1 expression, both immune cells and tumor cells, was assessed as well.

Synthesis of 18F-BMS-986192

18F-BMS-986192 was synthesized as per prior publication *(12-13)* at the GMP lab of the Department of Radiology & Nuclear Medicine of the Amsterdam University Medical Centre. 18F-BMS-986192 synthesis resulted in > 95% radiochemical purity and in 3-7% radiochemical yield and a molar activity of > 6.1 GBq/µmol.

Scan protocol

The PET/CT study was performed on a Philips Gemini TF-64 or an Ingenuity TF-128 PET/CT scanner (Philips Healthcare, Best, the Netherlands). The scan protocol started with a low-dose CT scan (120 kV, 30 mAs). The CT scan was followed by injection of a mean dose of 162±37 MBq 18F-BMS-986192, and subsequent 60-min single bed position PET scan. The field of view (FOV) was positioned over the chest and included the ascending aorta.

Afterwards, a whole body PET-CT scan (3 min per bed-position, 10–12 bed positions, depending on the height of the patient) from the vertex to mid-thigh was acquired. The 60 min single bed dynamic scan was reconstructed into 19 time frames (1x15, 3x5, 3x10, 4x60, 2x150, 2x300, 4x600 seconds) with BLOB-TOF-OSEM into a 144x144 matrix size with 4x4x4 mm^3 voxels.

Volumes of interest

Images were read by a nuclear medicine physician (DO) and areas of tumor uptake (defined as focal uptake exceeding local background) were identified. Volumes of interest (VOI) were delineated either semi-automatically or manually with the ACCURATE tool *(16)* on the dynamic PET scans. Tumor VOIs were delineated on the sum of the last four frames (representing the time average tumor uptake at 20 to 60 min post injection (p.i.)). A blood pool VOI was defined on the sum of frame 6-10 (representing the uptake at 50 to 290 seconds p.i.), in 4 transversal planes located at the aortic arch and part of the ascending aorta. Per plane the complete aorta was delineated. The tumor and blood pool VOI were used to derive tumor and blood time activity curves (TAC; based on the mean activity concentration in the VOI) from the dynamic PET data. In addition, the tumor VOIs were imported to the static PET scan.

Blood sampling

In addition to the dynamic scanning, continuous arterial sampling was performed at 5 mL min^{-1} during the first 5 minutes and 2.5 mL min^{-1} until the end of the first (single bed position) PET scan, using a dedicated on-line blood sampler *(17)*. Continuous sampling was interrupted at 5, 10, 20, 30, 40 and 60 min p.i. in order to draw 7 mL arterial blood. For all arterial blood samples, whole blood and plasma activity concentrations were measured with a well counter (Wallac1480 Wizard, Perkin Elmer, Waltham, USA).

In six patients, manual venous samples were drawn simultaneously with the arterial samples and processed similarly as the arterial samples. The venous over arterial whole body concentrations were obtained as a function of time. In addition, the venous whole blood over plasma ratios were compared to the arterial whole blood over plasma ratios.

Blood sampler derived input functions (BSIF)

The continuously sampled arterial whole blood activity concentration was recalibrated to the manual arterial samples and corrected for the arterial plasma / whole blood activity concentration ratio as well as for delay in order to obtain the BSIF.

Image derived input functions (IDIF)

Blood pool VOI derived whole blood time activity curves were multiplied with the arterial plasma / whole blood activity concentration ratios as well as delay in order to obtain the IDIF.

Pharmacokinetic analysis of 18F-BMS-986192

Pharmacokinetic modeling was performed using in-house developed software in MATLAB (MathWorks Inc, Natick, MA). 18F-BMS-986192 tumor TACs were analyzed using both irreversible and reversible one and two tissue compartment models in combination with the BSIF. All models included a delay term between BSIF and TAC as well as an additional blood volume fraction fit parameter.

The quality of the fit was assessed visually and the optimal compartment model was chosen based on the Akaike criterion *(18)*. Based on the optimal model, the preferred parameter to quantify tracer uptake was determined. Subsequently, the optimal compartment model was applied to the tumor TAC in combination with the IDIF. The preferred parameter estimate obtained with the IDIF was compared to the estimate obtained with the BSIF. All values reported from compartmental modeling were obtained with the optimal compartmental model.

The use of simplified uptake measures was explored by comparing these measures with the preferred fully quantitative parameter. Simplified uptake measures included SUV normalized to plasma concentration, SUV normalized to injected activity over body weight or lean body mass (SUV_{BW} and SUV_{LBM}) at 50 min p.i. and SUV_{BW} and SUV_{LBM} at 80 min p.i.

Statistical analysis

Each simplified variable was tested for correlation with the parameter derived from full kinetic modeling by linear regression analysis (R^2) using Graphpad Prism, version 6.02.

Results

Patients, lesions and biopsies

Nine patients, with a total of 22 lesions, were enrolled in this study. Six of the biopsied lesions were in the FOV of the dynamic scan. Three lesions with a volume smaller than 1 mL were excluded from the analysis. Another lesion was too close to a blood vessel, resulting in a lesion TAC that was dominated by spill-over from the vessel. In total, 18 lesions from 9 patients were available for kinetic modeling (Table 1). For six lesions the PD-L1 immunohistochemistry score in the biopsy was known: Three biopsies were negative for PD-L1, and three biopsies were positive for PD-L1 immunohistochemistry (tumor proportion score 10%, 90% and 95%, respectively).

Tumor TAC and blood sampling

Figure 1 shows the TAC for the six lesions with a biopsy derived PD-L1 score. In general, TACs for PD-L1 positive lesions were increasing over time, whereas the TAC for PD-L1 negative tumors remained more or less flat after 40 minutes post-injection. Figure 2 shows the comparison of arterial and venous blood sample derived activity concentrations and Figure 3 shows an example of the blood sampler derived arterial input function. Panel A shows venous / arterial whole blood concentrations as a function of time. The venous plasma / whole blood ratios correlated well with the arterial ratios (R^2 = 0.99), with a slope of 1.01 (panel B). The whole body PET-CT scan started at 67 +/- 1 min post injection (average +/- SD).

Kinetic modeling

Four conventional pharmacokinetic models were used: the single-tissue irreversible model, the single-tissue reversible model, the two-tissue irreversible model and the two-tissue, reversible model. All models included a blood volume fraction as fit parameter. Fits were visually assessed for goodness of fit. The Akaike criterion was used to determine the preferred model for tumor tracer uptake. Based on this criterion TAC were best described by a reversible single tissue model in 11 lesions (61%), followed by the irreversible two tissue model in seven lesions (39%; see Table 1). Although in these 7 lesions the irreversible model was preferred, it was seen that the single tissue reversible model still resulted in good fits (Figure 4B) and that the obtained VT estimates well correlated with other (simplified) uptake metrics. The preferred parameter to quantify tracer uptake was therefore the distribution

volume V_T, which ranged from 0.4 to 4.8 mL·cm^{-3} (see Table 1). In this table, also the fitted blood volume fraction is indicated. In all cases it was below 35% and did not affect quality of the fits nor the ability to obtain reliable estimates for the other fit parameters.

A typical example of a fitted TAC of a PD-L1 positive and a PD-L1 negative tumor is shown in Figure 4. For these 6 fits, one PD-L1 negative and the 10% PD-L1 positive lesion showed, based on the Akaike criterion, a preference for the two tissue irreversible model. The other four showed a preference for the single tissue reversible model. The volume of distribution for the PD-L1 negative lesions was lower than 1, whereas V_T for the PD-L1 positive lesions was larger than 1 and increasing with the immunohistochemistry score (see Table 1). Replacing the BSIF with the IDIF provided similar V_T results (Figure 5; the correlation line has a slope of 0.99 and an R^2 of 0.98; Panel B shows an example blood pool VOI).

Simplified analysis

V_T derived from the reversible single tissue model in combination with the BSIF was used for the validation of simplified methods. SUV normalized for body weight 50 min p.i. correlated best with V_T (R^2= 0.92, Figure 6a), followed by SUV normalized for body weight at 80 min p.i. (R^2=0.91, Figure 6b), SUV normalized for lean body mass 50 min p.i. (R^2=0.90, Figure 6c) and SUV normalized to plasma concentration (R^2=0.84).

Discussion and Conclusion

In this study, we performed a full pharmacokinetic analysis of 18F-BMS-986192 with a dynamic scanning protocol and arterial blood activity input. A metabolite analysis of the tracer was not performed since it has been shown that in mice no metabolites were found within 2h after injection (*12*). Although tracer uptake seemed to be still increasing with time at the end of the dynamic scan interval, at 60 minutes p.i. a reversible single tissue model best described the uptake of 18F-BMS-986192 in 61% of the tumors. An irreversible two tissue model was preferred in 39% of the fits, notably in one lesion with a 10% positive immunohistochemistry score and in one lesion with a negative immunohistochemistry score. Consequently, the distribution volume was found to be the preferred parameter for the tumoral PD-L1 uptake. This parameter was higher for PD-L1 (biopsy) positive tumors than for negatively scored lesions, based on the six lesions for which immunohistochemistry data were available. However, the small number of tumor tissues in which PD-L1 was determined precludes the drawing of firm conclusions regarding the relation between tracer uptake and immunohistological expression of PD-L1.

Full kinetic modeling with a BSIF is the preferred method for tracer uptake quantification. Given the burden of arterial sampling, the use of an IDIF was explored and the resulting V_T values correlated closely to those obtained with the BSIF. However, a significant variation of plasma to whole blood ratio was observed. Therefore, arterial sampling is not needed for the quantification of this tracer when the ascending aorta is in the FOV, but at least one venous sample is needed to correct for the patient specific plasma to whole blood ratio. In a next step, the accuracy of simplified measurements based on a shortened scan protocol was explored. In this study, we found that SUV_{BW} correlated best with V_T. This validates the use of SUV_{BW} to quantify uptake of 18F-BMS-986192 as e.g. used in (*13*). It is important to note that the relationship between the bioavailability of the tracer and the uptake of the tracer in tumor tissue may be influenced by concurrent medication or other interventions. Therefore, in the setting of monitoring of response to anti-PD-(L)1 therapy, it will be important to confirm the appropriateness of the single tissue reversible model to describe the adnectin uptake, as well as the validation of SUV against V_T.
Given the rise in uptake in PD-L1 positive lesions the results of this paper cannot be readily applied to simplified measures (SUV) at other time intervals than 50 to 80 min p.i. Moreover, it suggests the importance of adhering to strict standardized uptake time intervals in case static whole body imaging is performed.

In conclusion, the result of this study allows for clinical implementation and quantification of the 18F-BMS-986192 PD-L1 PET tracer uptake in baseline studies. A single tissue reversible compartment model describes the kinetics of 18F-BMS-986192 uptake in lesions. SUV_{BW} at 60 minutes post injection seems to be a good surrogate to quantify tumor tracer uptake for baseline PET studies. To assess its value for response evaluation during PD-(L)1 immune checkpoint inhibition, dynamic scanning combined with an image derived input function and at least one blood sample would allow to expand the present results to this setting.

Disclosure Statement

Potential conflicts of interest: DL and WH are employees and stock holders of BMS

Financial disclosure: not applicable

KEY POINTS

QUESTION: How to quantify PDL-1 expression based on 18F-BMS-986192 PET/CT

PERTINENT FINDINGS: This methodological paper applied kinetic modeling to tissue and plasma time activity curves of baseline NSCLC patients. A single compartment reversible model, or SUV_{BW} at 60 min p.i. as simplified measure should be used.

IMPLICATIONS FOR PATIENT CARE: Dynamic scanning combined with an image derived input function and at least one blood sample allow to investigate the role of 18F-BMS-986192 PET/CT in response evaluation during PD-(L)1 immune checkpoint inhibition therapy.

References

1. Ferlay J, Soerjomataram I, Dikshit R, et al. Cancer incidence and mortality worldwide: sources, methods and major patterns in GLOBOCAN 2012. *Int J Cancer*. 2015;136:E359-386.

2. Borghaei H, Paz-Ares L, Horn L, et al. Nivolumab versus docetaxel in advanced nonsquamous non-small-cell lung cancer. *N Engl J Med*. 2015;373:1627-1639.

3. Herbst RS, Baas P, Kim D-W, et al. Pembrolizumab versus docetaxel for previously treated, PD-L1-positive, advanced non-small-cell lung cancer (KEYNOTE-010): a randomised controlled trial. *Lancet*. 2016;387:1540-1550.

4. Rittmeyer A, Barlesi F, Waterkamp D, et al. Atezolizumab versus docetaxel in patients with previously treated non-small-cell lung cancer (OAK): a phase 3, open-label, multicentre randomised controlled trial. *Lancet*. 2017;389:255-265.

5. Shukuya T, Carbone DP. Predictive markers for the efficacy of anti-PD-1/PD-L1 antibodies in lung cancer. *J Thorac Oncol*. 2016;11:976-988.

6. Sacher AG, Gandhi L. Biomarkers for the clinical use of PD-1/PD-L1 inhibitors in non-small-cell lung cancer: a review. *JAMA Oncol*. 2016;2:1217-1222.

7. Ilie M, Long-Mira E, Bence C, et al. Comparative study of the PD-L1 status between surgically resected specimens and matched biopsies of NSCLC patients reveal major discordances: a potential issue for anti-PD-L1 therapeutic strategies. *Ann Oncol*. 2016;27:147-153.

8. Hellmann MD, Ciuleanu T-E, Pluzanski A, et al. Nivolumab plus ipilimumab in lung cancer with a high tumor mutational burden. *N Engl J Med*. 2018;378:2093-2104.

9. Hellmann MD, Callahan MK, Awad MM, et al. Tumor mutational burden and efficacy of nivolumab monotherapy and in combination with ipilimumab in small-cell lung cancer. *Cancer Cell*. 2019;35:329.

10. Taube JM, Klein A, Brahmer JR, et al. Association of PD-1, PD-1 ligands, and other features of the tumor immune microenvironment with response to anti–PD-1 therapy. *Clin Cancer Res*. 2014;20:5064-5074.

11. Lammertsma AA. Forward to the past: the case for quantitative PET imaging. *J Nucl Med*. 2017;58:1019-1024.

12. Donnelly DJ, Smith RA, Morin P, et al. Synthesis and biologic evaluation of a novel 18F-labeled adnectin as a PET radioligand for imaging PD-L1 expression. *J Nucl Med*. 2018;59:529-535.

13. Niemeijer AN, Leung D, Huisman MC, et al. Whole body PD-1 and PD-L1 positron emission tomography in patients with non-small-cell lung cancer. *Nat Commun*. 2018;9:4664.

14. Clinical Trials register - Search for 2015-004760-11. https://www.clinicaltrialsregister.eu/ctr-search/search?query=2015-004760-11, accessed on January 28th 2020.

15. Thunnissen E, de Langen AJ, Smit EF. PD-L1 IHC in NSCLC with a global and methodological perspective. *Lung Cancer*. 2017;113:102-105.

16. Boellaard R. Quantitative oncology molecular analysis suite: ACCURATE. *J Nucl Med*. 2018;59:1753-1753.

17. Boellaard R, van Lingen A, van Balen SC, Hoving BG, Lammertsma AA. Characteristics of a new fully programmable blood sampling device for monitoring blood radioactivity during PET. *Eur J Nucl Med*. 2001;28:81-89.

18. Akaike H. A new look at the statistical model identification. *IEEE Transactions on Automatic Control*. 1974;19:716-723.

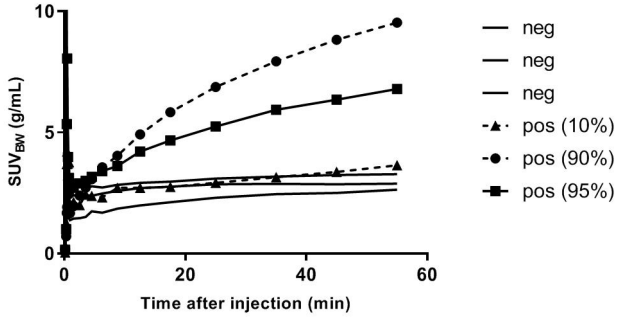

FIGURE 1. Time activity curves for PD-L1 positive (red) and PD-L1 negative (black) tumors

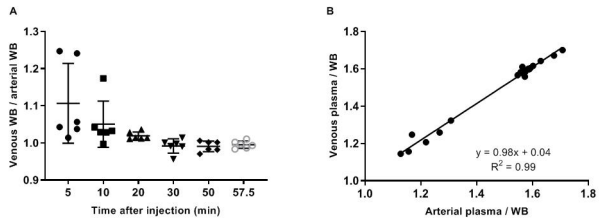

FIGURE 2. Comparison of arterial and venous blood derived activity concentrations. Panel A shows the observed venous over arterial whole blood (WB) concentration ratios as a function of time p.i. Panel B shows venous whole blood over plasma ratios as a function of arterial whole blood over plasma ratios.

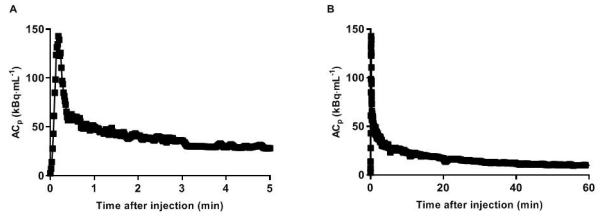

FIGURE 3. Example blood sampler derived input. Panel A shows the first 5 minutes, Panel B the full BSIF

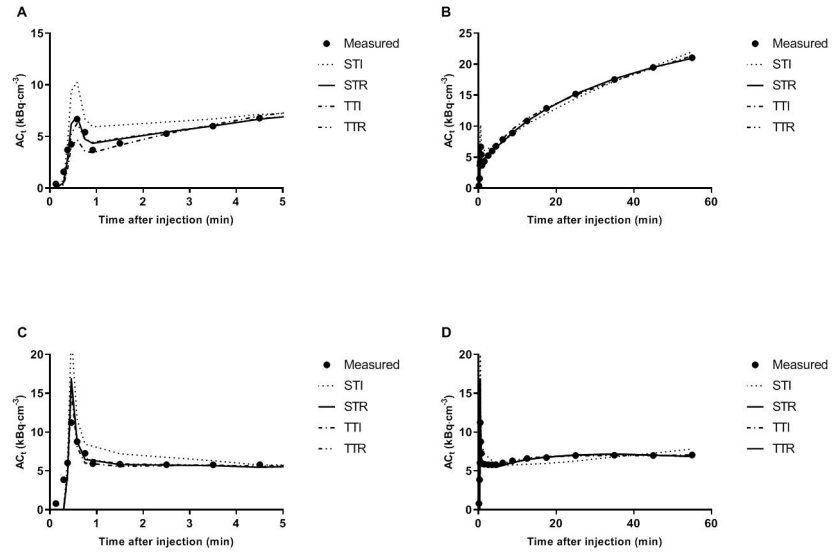

FIGURE 4. Example fitted time activity curve for PD-L1 positive (Panel A for the first 5 and Panel B for the full duration of the time activity curve) and a PD-L1 negative (Panel C for the first 5 and Panel D for the full duration of the time activity curve) tumors with single tissue (reversible (STR) and irreversible (STI)) and two tissue (reversible (TTR) and irreversible (TTI)) compartmental model fits to the data.

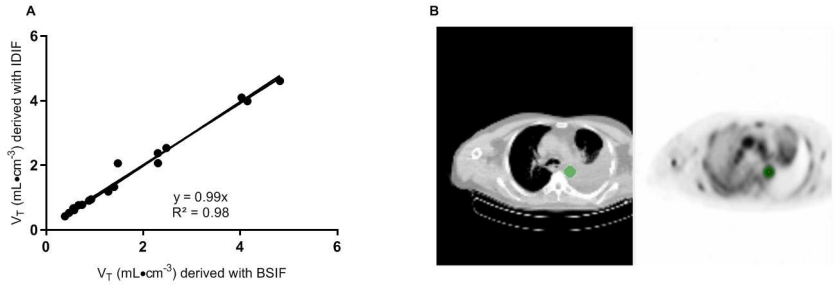

FIGURE 5. Correlation of V_T values derived with the use of a blood sampler (BSIF) or image derived (IDIF) input function (Panel A). In Panel B an example blood pool VOI is shown as delineated on the sum of frame 6-10 (representing the uptake at 50 to 290 seconds p.i.).

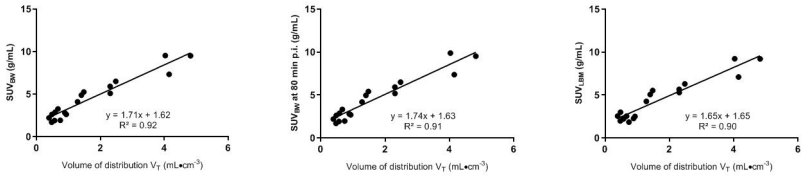

FIGURE 6. Correlation of $SUV_{r,plasma}$ (Panel A), SUV_{LBM} (Panel B) and SUV_{BW} at 50 min p.i. (Panel C) and SUV_{BW} at 80 min p.i. (Panel D) with V_T from the single tissue reversible model.

TABLE 1. Tumors in FOV

patient	localization	#	volume (mL)	Tumor PD-L1 expression from IHC	Total PD-L1 in slide %	Model preference AIC	V_T mL·cm^{-3}	V_b (%)
2	Lung RLL	1	77.7	+ (90%)	25%	STR	4.0	10
2	LN 10R	2	4.1	N.A.		STR	4.1	31
2	LN 4R	3	5.7	N.A.		STR	4.8	14
2	Lung LLL	4	86.0	+ (95%)	64%	STR	2.5	17
3	Lung LLL	1	59.1	- (0%)	2%	TTI	0.6	17
6	Lung RUL	1	2.3	N.A.		STR	0.7	8
7	LN AXIL 1	1	6.4	N.A.		STR	0.7	7
7	LN N7	2	24.7	N.A.		TTI	2.3	20
7	LN AXIL 2	3	14.5	- (0%)	3%	STR	0.9	10
8	Lung RUL	1	6.4	N.A.		STR	0.6	11
8	Humerus	2	18.0	N.A.		TTI	0.5	7
9	Lung RUL	1	68.5	- (0%)	5%	STR	0.9	22
11	Lung Hilar mass	2	6.5	N.A.		STR	1.5	22
12	Lung LLL	1	2.4	+ (10%)	10%	TTI	1.3	16
12	LN 10L	2	1.2	N.A.		TTI	1.4	34
12	LN 11L	3	2.7	N.A.		STR	2.3	34
13	PANCREAS	1	8.8	N.A.		TTI	0.4	11
13	PANCREAS	2	26.6	N.A.		TTI	0.5	15

RLL right upper lobe, LN Lymph node, LLL Left lower lobe, RUL right upper lobe, AXIL axillary, IHC immunohistochemistry, STR = single tissue reversible, TTI = two tissue irreversible, V_T = volume of distribution (mL•cm^{-3}), V_b = blood volume fraction (%).